CAIT-UTC-NC17

Piezoelectric Energy Harvesting in Airport Pavement

FINAL REPORT
August 2019

Submitted by:

Hao Wang
Associate Professor

Jingnan Zhao
Graduate Research Assistant

Rutgers, The State University of New Jersey
96 Frelinghuysen Road, Piscataway, NJ, 08854

External Project Manager
Navneet Garg, FAA

In cooperation with

Rutgers, The State University of New Jersey
And
Federal Aviation Administration
And
U.S. Department of Transportation
Federal Highway Administration

Disclaimer Statement

The contents of this report reflect the views of the authors, who are responsible for the facts and the accuracy of the information presented herein. This document is disseminated under the sponsorship of the Department of Transportation, University Transportation Centers Program, in the interest of information exchange. The U.S. Government assumes no liability for the contents or use thereof.

The Center for Advanced Infrastructure and Transportation (CAIT) is a National UTC Consortium led by Rutgers, The State University. Members of the consortium are the University of Delaware, Utah State University, Columbia University, New Jersey Institute of Technology, Princeton University, University of Texas at El Paso, Virginia Polytechnic Institute, and University of South Florida. The Center is funded by the U.S. Department of Transportation.

1. Report No.	2. Government Accession No.	3. Recipient's Catalog No.
CAIT-UTC-NC17		

4. Title and Subtitle	5. Report Date
Piezoelectric Energy Harvesting in Airport Pavement	August, 2019
	6. Performing Organization Code CAIT/Rutgers University

TECHNICAL REPORT STANDARD TITLE PAGE

7. Author(s)	8. Performing Organization Report No.
Hao Wang, PhD, and Jingnan Zhao	CAIT-UTC-NC17

9. Performing Organization Name and Address	10. Work Unit No.
Rutgers, The State University of New Jersey 96 Frelinghuysen Road, Piscataway, NJ, 08854	11. Contract or Grant No. DTRT13-G-UTC28

12. Sponsoring Agency Name and Address	13. Type of Report and Period Covered
Center for Advanced Infrastructure and Transportation Rutgers, The State University of New Jersey 100 Brett Road Piscataway, NJ 08854	Final Report 1/1/2015– 9/30/2019
	14. Sponsoring Agency Code

15. Supplementary Notes

U.S. Department of Transportation/OST-R
1200 New Jersey Avenue, SE
Washington, DC 20590-0001

16. Abstract

This study investigates the potential of applying piezoelectric energy harvesting technology in airfield pavements, which can provide electricity for smart sensors and LED lights at airfield. The energy harvesting performance of piezoelectric transducers was evaluated based on mechanical energy induced by aircraft loading on taxiway and runway. Stacked piezoelectric transducer design was used in this study to estimate the power output of piezoelectric harvester embedded in wheel path. Three-dimensional finite element models were used to calculate stress pulses and magnitudes under different loading conditions. The critical pavement responses of flexible pavement related to fatigue cracking, shear failure, and rutting were analyzed. The simulation results quantified the expected energy generation and dynamic responses of flexible pavements at different aircraft loads, speeds, and pavement temperatures. The results provide suggestions for optimizing installation of energy harvester in airfield pavements.

17. Key Words	18. Distribution Statement
Piezoelectric energy harvesting, flexible pavement, pavement responses, finite element model, power output	

19. Security Classification (of this report)	20. Security Classification (of this page)	21. No. of Pages	22. Price
Unclassified	Unclassified	Total #39	

Form DOT F 1700.7 (8-69)

Table of Contents

List of Figures

List of Tables

Section 1: Introduction

1.1 Problem Statement

Energy harvesting is a promising technique that can help solve global energy challenge without depleting natural resources. Federal, state, and local governments have enacted renewable energy policy to mitigate potential impacts of climate change and invest in long-term economic savings associated with renewable energy. Solar, geothermal, biomass, and wind have been utilized to harvest energy in different airport projects (Whiteman et al., 2015).

In recent years, piezoelectric technology has been used to convert the available mechanical energy potential in pavement into electrical energy, which has been widely used in roadways and bridges. The voltage produced from piezoelectric material varies with time and results in an alternate current (AC) signal, which causes the direct and inverse piezoelectric effect, respectively. Piezoelectric technology has advantages over the other energy harvesting technologies in infrastructure: it can be used for both energy harvesting and pavement structure sensing, which will be quite beneficial for smart infrastructure. The challenge of using piezoelectric technology for energy harvesting is to integrate the piezoelectric transducer with the structure of roadway and bridges. The energy harvesting performance of piezoelectric transducers (PZTs) is affected by material, geometry design of transducer, and external loading.

Previous studies have investigated the feasibility of applying piezoelectric energy harvester on roadways and bridges to generate electric energy effectively for different uses. However, few works have been conducted to investigate the potential of using piezoelectric energy harvesting at airport for green energy solutions. Airfield pavements are designed to carry repeated loading of heavy aircraft. Therefore, research is needed to explore the potential of harvesting energy in airport infrastructure using piezoelectric technology.

1.2 Objective and Scope

This study investigated the potential of applying piezoelectric energy harvesting technology in airfield pavements. The energy harvesting performance of piezoelectric transducers was evaluated based on mechanical energy induced by multi-wheel aircraft loading on taxiway and runway. A 3D FE model was used to estimate the stress pulse and magnitude under moving aircraft tire loading. Stack piezoelectric transducer design was used in this study to estimate the energy power output of energy harvester embedded in the pavement. The impact of energy harvester on critical pavement responses related to fatigue cracking and rutting were analyzed.

Section 2: Literature Review

2.1 Principles of Piezoelectric Energy Harvesting

Piezoelectric materials generate an electric charge when subjected to mechanical stress, and change dimensions when an electric field is applied across the material. These are known respectively as the direct and the inverse piezoelectric effect (Cobbold, 2006). Piezoelectric materials can be classified into the following categories: 1) single crystalline material (as quartz); 2) piezoceramics (as PZTs); 3) piezoelectric semiconductor (as ZnO2); 4) polymer (as PVDF); 5) piezoelectric composites; and 6) glass ceramics (as Li2Si2O5, Ba2TiSiO6). Also, PZT fibers can be mixed with resin to form macro fiber composite (MFC) or PZT composite. The mechanical and piezoelectric properties vary among these different piezoelectric materials. PZT material has been used in many applications among commercial products due to the high efficiency of electricity generation.

Increasing the applied stress or strain on piezoelectric material that provides more mechanical energy is one of the main methods to increase the generated power. The other method is to use the coupling mode more efficiently. Figure 1 shows two possible coupling methods of piezoelectric material; the d31 and d33 mode, depending on material poling and applied force directions. The coupling mode is dependent on the relationship between the direction of the applied load and the poling direction. The coupling mode is d33 mode when the applied load is parallel to the poling direction;

while the d31 mode is defined when the applied load is perpendicular to the poling direction. The d33 mode provides higher electromechanical coupling when compared with the d31 mode for most typical piezoelectric materials (Anton and Sodano, 2007).

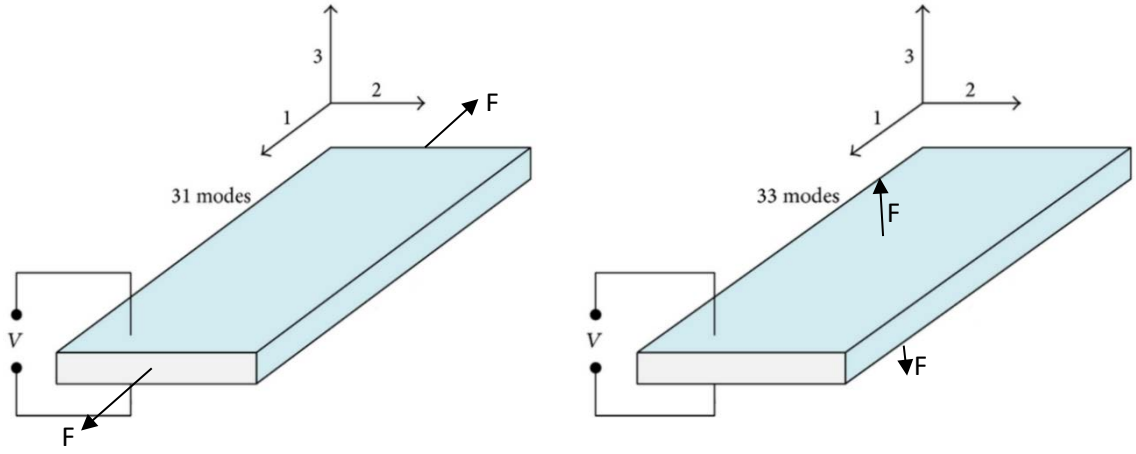

Figure 1 Piezoelectric material coupling modes (after Roundy et al. 2003).

The piezoelectric charge constant (effective piezoelectric strain constant), and the piezoelectric voltage constant are governing the magnitude of energy conversion. Quality factor is another important factor of piezoelectric material because the greater quality factor indicates the less damping and heat generation during energy conversion. In order to increase the efficiency of piezoelectric energy harvesting, the preferred material properties are higher piezoelectric coefficient, higher quality, and lower elastic compliance.

The density of stored electric energy can be obtained using Equation 1. It can be concluded that UE is related to (d·g) value if external stress is constant. Therefore, the PZT materials with a high (d·g) value are improved for energy harvesting.

$$\boldsymbol{U_E = \frac{1}{2} dgT^2} \quad (1)$$

Where, U_E is the density of electric energy, d is the piezoelectric strain constant, g is the piezoelectric voltage constant, and T is the external stress.

The most frequently used piezoelectric transducer in pavement applications is disk/rod shaped PZT transducers due to its durability and easy fabrication, as shown in Figure 2. The transducer has two main geometric variables which are diameter and thickness. As the diameter-to-thickness ratio is equal to or more than 5, it is usually called disk-shape. The geometry of PZT affects the stress applied on the top surface of transducer and thus the harvested energy. In order to optimize disk/rod geometry for energy harvesting application, the diameter-to-thickness ratio need be adjusted.

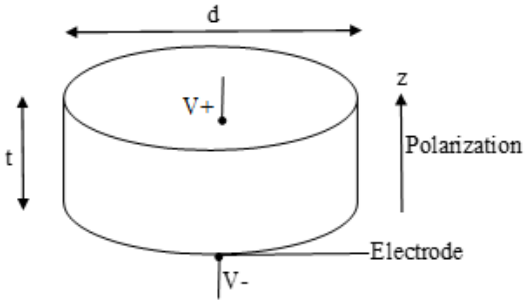

Figure 2 Illustration of disk/rod shaped PZT transducer

2.2 Review of Relevant Studies

Previous studies have utilized or combined laboratory tests, field tests, and mathematical models to investigate the feasibility of placing PZTs in pavements to produce electric power for sensors and utilities in infrastructure.

Roshani and Dessouky (2015) used a ceramic disk-shaped PZT fit amongst two copper plates in asphalt mixture. They analyzed the influence of a list of parameters, including pavement thickness, traffic speed and load, on electronic voltage output and found that greater loads and smaller loading durations were able to substantially boost output voltages. Jasim et al. (2019) estimated the modulus of energy harvester using lab tests of which the results were consistent with those derived from the finite element (FE) models.

Xiang et al. (2013) used a theoretical method, in which infinite Bernoulli-Euler beam was built on a Winkler basis, to examine the piezoelectric effects caused by pavement deformation and stated that vehicle speed and pavement conditions had impacts on the account of energy collected by PZ materials. The electric power output of these materials was found at their peak at a specific vehicle speed. They switched to utilize Kirchoff plate model to analyze the impacts of the transducer position and wheel load distributions on the electric power output, particularly in the soft subgrade scenario (Zhang et al., 2016). Jiang et al. (2014) created a two-degrees-of-freedom piezoelectric model for a piezoelectric harvester made of three stacks per unit. The

electromechanical model and experimental results proved that the energy harvester was able to produce electric power for electrical devices in infrastructure.

Xiong (2014) examined six fabricated energy harvesters using a plate-over-pillar design in pavement at the I-81 Troutville weigh station. A disk shape was selected to reduce the possibility of damage from piezoelectric materials, and disk spacing was changed to limit the material stress involved. Prior to its implementation in the field, lab tests were conducted to confirm the damage resistance and electric output of the piezoelectric materials, while field tests were also completed to confirm environmental durability. It was found that power produced by the piezoelectric energy harvesters at the Troutville weigh station have dramatic drops after 12 months.

The rechargeable battery and the supercapacitor are the energy storage devices most widely employed to gather PZT electricity (Sodano et al., 2005; Xiong, 2014). Generally, supercapacitors were more appropriate for storing energy than rechargeable batteries in piezoelectric energy harvesting system when considering energy efficiency, self-discharge rate, energy density and lifetime (Ottman et al., 2002; Guan and Liao, 2008; Hadjipaschalis et al., 2009). To produce the greatest amount of power possible in random traffic conditions, a diode rectifier should be involved to link with PZT cells. Loading resistors need to be used to change the voltage on the charging supercapacitor.

Section 3: Pavement Models with Piezoelectric Energy Harvester

3.1 Pavement Structure and Material Properties

An advanced 3D-FE model of flexible pavement, which was validated in the previous works, was simulated using software ABAQUS Version 6.13-EF2 (Dassault Systèmes). In the model, eight-node, linear brick elements with reduced integration were used in the finite domains, while infinite elements were used at boundaries to reduce many far-field elements without significant loss of accuracy. Figure 3 illustrates the 3-D FE model and cross-section of the flexible pavement structure. Pavement structure consists of asphalt concrete layer (254 mm in thickness), aggregate based layer (381 mm in thickness), and sandy subgrade. The FE mesh is refined through sensitivity analysis considering the balance between model accuracy and computation time. The final selected domain size, including finite and infinite sections, has an in-plane dimension of 6000×9000 mm and a vertical dimension of 4000mm. More details on the model can be found in the authors' previous works (Wang et al., 2015; Wang et al., 2016).

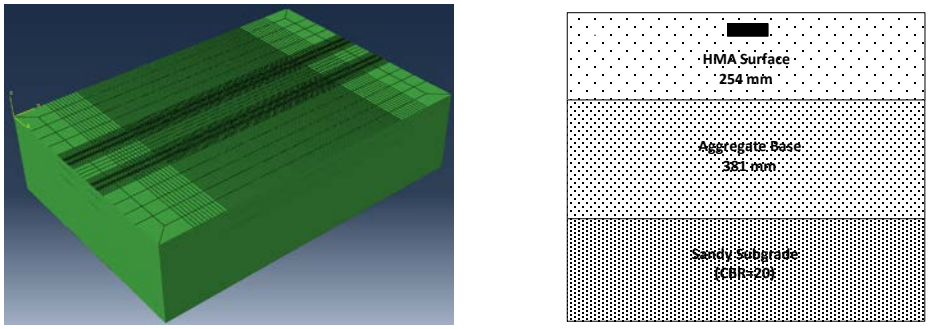

Figure 3 Modeled pavement: 3D FE model (left) and cross-section structure (right)

The aircraft tire loading on taxiing runway after landing was simulated using moving load under the non-uniform distribution of contact stresses at the tire-pavement interface. The landing gear located at one side of the fuselage was considered in the simulation. For each tire inflation pressure, the distribution of contact stresses was assumed non-uniform under the tire imprint with five ribs. The non-uniformly distributed vertical contact stress distributions were estimated based on the contact stress measurements under heavy aircraft tire loading in the previous work (Rolland, 2009). In the longitudinal direction, a half-sinusoidal distribution of vertical contact stress along the contact length of each rib was utilized. It was assumed that the peak contact stresses under tow edge ribs were 2.5 times the tire inflation pressure, and the peak contact stresses under central ribs were 1.2 times the tire inflation pressure. The contact width was assumed unchanged due to the high lateral stiffness of the tire sidewall. The contact length decreased as the tire inflation pressure increased. The distribution of vertical contact stress with tire inflation pressure of 1.40 MPa presents a concentrated stress as high as 2.1 MPa at the edge ribs and 1.40 MPa at the central ribs. The maximum landing weight of B737-800 (154 kN) was assumed to investigate the application of piezoelectric energy harvester at taxiway, high-speed taxiway and runway (Brady, 1999). The simulated speeds at regular taxiway, high speed taxiway and runway were 8 km/h (5 mph), 48 km/h (30 mph), and 96 km/h (60 mph), respectively.

The viscoelastic material properties of asphalt mixture were considered in the FE model. Dynamic modulus tests were conducted at different temperatures and loading frequencies for the asphalt mixture in the testing sections. Table 1 shows Prony series parameters for asphalt layer at the reference temperature of 20°C. The relaxation modulus was inter-converted from dynamic modulus using Equation 2-3 assuming that the linear viscoelasticity of HMA was represented by a generalized Maxwell solid model (Park and Kim, 1999). The bulk and shear relaxation moduli were calculated assuming a constant Poisson's ratio. The relationship between the shift factor and the temperature can be approximated by the Williams-Landell-Ferry (WLF) function as expressed in Equation 5.

$$E^{'}(\omega) = E_{\infty} + \sum_{i=1}^{n} \frac{\omega^2 \tau_i^2 E_i}{1 + \omega^2 \tau_i^2} \tag{2}$$

$$E^{''}(\omega) = \sum_{i=1}^{n} \frac{\omega \tau_i E_i}{1 + \omega^2 \tau_i^2} \tag{3}$$

$$\min \sum_{j=1}^{k} \left[\left(\frac{E^{'}(\omega)_{calcualted}}{E^{'}(\omega)_{measured}} - 1 \right)^2 + \left(\frac{E^{''}(\omega)_{calculated}}{E^{''}(\omega)_{measured}} - 1 \right)^2 \right] \tag{4}$$

Where, $E^{'}(\omega)$ is real part of the dynamic modulus, $E^{''}(\omega)$ is imaginary part of the dynamic modulus, E_{∞} is equilibrium relaxation modulus at infinite time, ω is angular frequency, E_i, τ_i are Prony series parameters for relaxation modulus as shown in Table 1, n is number of Maxwell elements; and k is number of data points from the measurements.

$$\log(a_T) = -\frac{C_1(T - T_0)}{C_2 + (T - T_0)} \quad (5)$$

Where, T_0 is reference temperature, T is actual temperature corresponding to the shift factor; and C_1, C_2 are regression parameters.

Table 1 Viscoelastic parameters of asphalt concrete at 20°C

i	**E_i**	**τ_i**	**WLF Parameters**	
1	0.4388	0.00	C_1	35.63
2	0.3388	0.38		
3	0.1694	10.96		
4	0.0128	501.00		
5	0.0097	815.36	C_2	293.15
6	0.0184	6215.40		
7	0.0053	19200.08		

3.2 Embedment of Energy Module in Pavement

In the FE model, the piezoelectric energy harvester developed by Roshani et al. (2018) was embedded in flexible pavement structure to estimate the electric power output. The prototype consisted of two copper plates connected with electric wires, four cylindrical piezoelectric disks, and two polystyrene sheets. The thickness of the copper plates was 6.35 mm, and the diameter was 152 mm. The copper plates worked as electrodes connecting the piezoelectric disks in parallel. The polystyrene plates were used to hold the piezoelectric disks between the copper plates by cutting a symmetrical

distribution of holes in the polystyrene sheets. The thickness and diameter of piezoelectric disks were 8 mm. The piezoelectric disks were made from PZT and the piezoelectric charge constant of d33 was 290E-12 m/v. The density and Young's modulus of piezoelectric material was 7.6 g/cm^3 and 6.8E10 N/m^2. The total height of the proposed piezoelectric harvester was around 21 mm (around 1 inch).

It was expected that the location of piezoelectric harvester impacted the stress distribution in pavement structure and piezoelectric effects. Previous research has shown that 50.8 mm (2 inch) below pavement surface in asphalt concrete layer is a reasonable location to place the piezoelectric harvester (Roshani et al., 2018; Jasim et al., 2019). In this study, the piezoelectric harvester was assumed to be 50.8 mm below the pavement surface along the wheel path of aircraft (reference case). Considering tire wandering when aircraft is moving at taxiway and runway, three horizontal locations were considered in the FE model. The energy module was simulated to be embedded under the edge ribs of aircraft tires, under the center ribs of aircraft tires, and beside the wheel path.

Section 4: Power Output of Piezoelectric Energy Harvester

4.1 Compressive Stress on Energy Harvester

The stress magnitude and pulse time above energy module are related to electric power output of piezoelectric harvester. Figure 4 (a) shows the stress magnitudes and pulse time on top of the piezoelectric harvester as the harvester was embedded under the edge ribs (UnderE), center ribs (UnderC), and beside the aircraft tires (UnderS). The simulated aircraft speeds were 8 km/h and 48km/h and the temperature was 25°C and 40°C, respectively. The results indicated that the differences of loading pulses in the asphalt concrete layer with and without piezoelectric harvester could be neglected. The results showed that the compressive stresses in the pavement structure with the energy module buried under the edge ribs of aircraft tires were 18% larger than those with the energy module placed under the center ribs of aircraft tires. The compressive stresses above the energy module located beside the aircraft tires were significantly reduced. This indicates that the wandering of aircraft tire should be taken into account while estimating the energy power output.

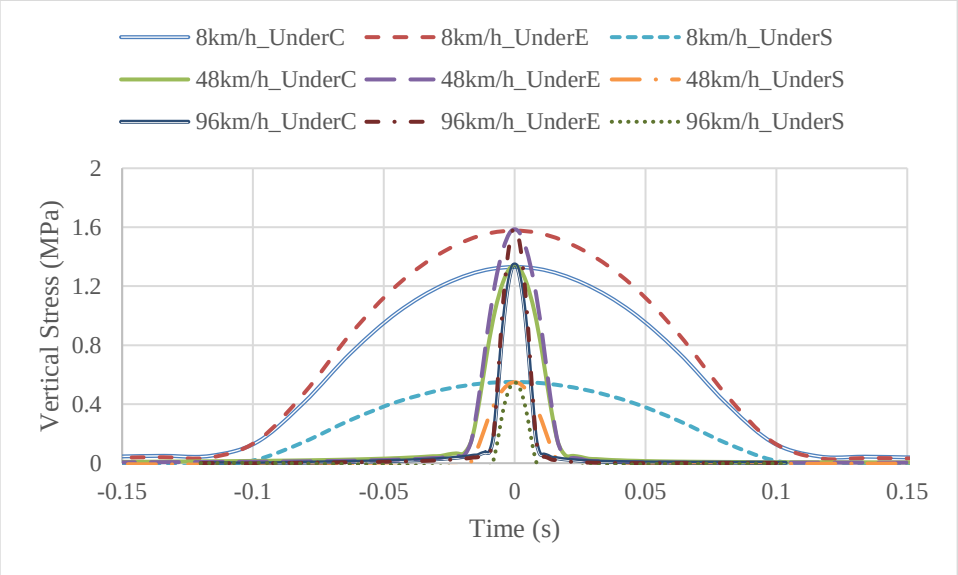

(a)

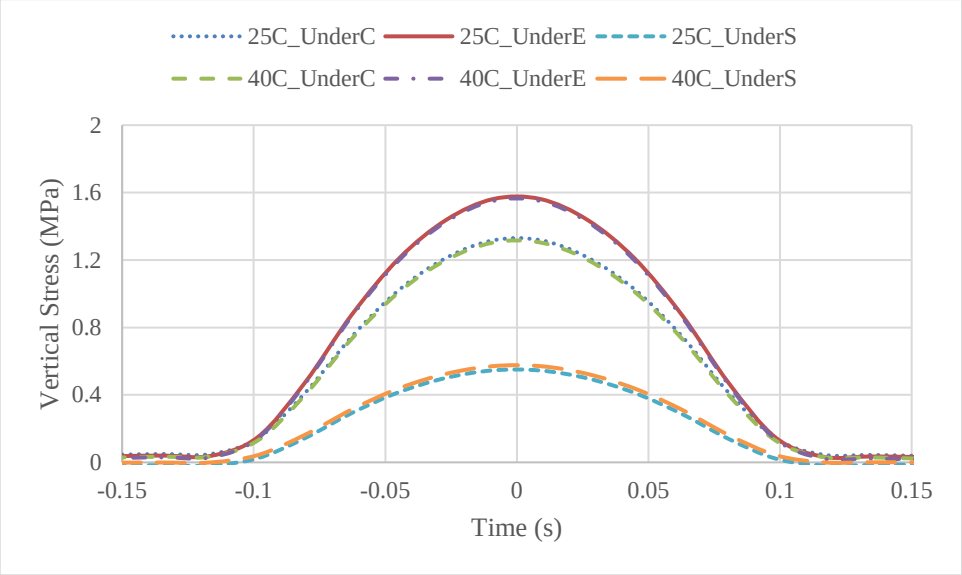

(b)

Figure 4 Stress magnitude and pulse time under moving load (a) at 8km/h, 48km/h, and 96 km/h (25°C); (b) at 25°C and 40°C (8km/h)

Figure 4 (b) presents the stress magnitudes and pulse time on top of the piezoelectric harvester as the harvester was embedded at different horizontal locations. The simulated temperatures were 25°C and 40°C. The results indicated that the increase of pavement temperature caused very small changes of compressive stress. Thus, the influence of changes in pavement temperatures could be considered negligible, which was similar to the results in Jasim et al. (2019). On the other hand, the temperature would not affect the functional performance of piezoelectric material when the temperature was lower than 150°C (Miclea et al. 2007).

4.2 Electric Power Generated by Piezoelectric Energy Harvester

The energy output of piezoelectric transducer is determined by the magnitude and frequency of excitation stress. For the piezoelectric energy harvester assumed in this study, a regression model has been developed based on laboratory testing to calculate the electric power output of each piezoelectric disk (Roshani et al., 2016; Roshani et al., 2018). The output power in the function of loading frequency and applying stress value was given by Equation 6.

$$\boldsymbol{P = a\sigma^{bf+c}} \tag{6}$$

Where, P is the output power (mW) of each piezoelectric disk, σ is the applied stress (MPa) on piezoelectric disk, f is the loading frequency (Hz), and a, b, and c are constant with values of 0.0068, 0.0164, and 1.89.

It is noted that the number of piezoelectric disks would affect the total power output under the same loading condition. To enhance the power output and cost-effectiveness, it was assumed that the energy module included four piezoelectric stacks, which resulted in the highest energy output in the previous study (Roshani et al., 2016). The electric power output generated by piezoelectric energy harvester was estimated using Equation 6 at the loading frequency of 5 Hz, 25 Hz, and 50 Hz for the speed of 8km/h, 48km/h, and 96km/h, respectively.

Table 2 summarizes the electric power output generated by one energy module under one aircraft tire considering three horizontal locations. It was assumed that the embedment was at one side of the wheel path. As expected, the horizontal locations of energy module in pavement influenced the electric power output. The power output was reduced by 12%-19% depending on speeds and temperature when the energy module was beneath the central ribs compared to the condition under the edge ribs. The power output was reduced to less than 2% as the tire completely deviated from the location of the buried energy module. The power output was affected by aircraft speed dramatically because of the exponential relationships between electric power output and speed.

Table 2 Electric power output of 1-inch energy module

(unit: mW per energy module)

Location of Energy Module	8 km/h		48 km/h		96 km/h	
	25°C	40°C	25°C	40°C	25°C	40°C
Edge Rib	859	858	4837	4825	42163	41836
Center Rib	739	752	4038	4087	33942	34251
Besides Tire	12	12	34	35	128	128

4.3 Effect of Location of Energy Module

Previous studies have stated that the embedment locations of energy module along pavement depth would have influence on compressive stresses above energy module and power output. Since the vertical compressive stresses decreased with the increase of depth within the pavement, it was recommended to place the energy module near pavement surface to maximize the energy power output. Three pavement depths of the top surface above energy module, including 25.4 mm, 50.8 mm and 76.2 mm, were considered and compared in the study. Figure 5 presents the in-depth distribution of vertical stresses on top of the energy module while the energy module was placed at different pavement depths. The simulated aircraft speed and temperature were 8 km/h and 25°C, respectively. The stress magnitude decreased significantly but the pulse time increased slightly as the energy module was buried deeper in pavement structure, which was induced by the moving pattern of aircraft tire loads.

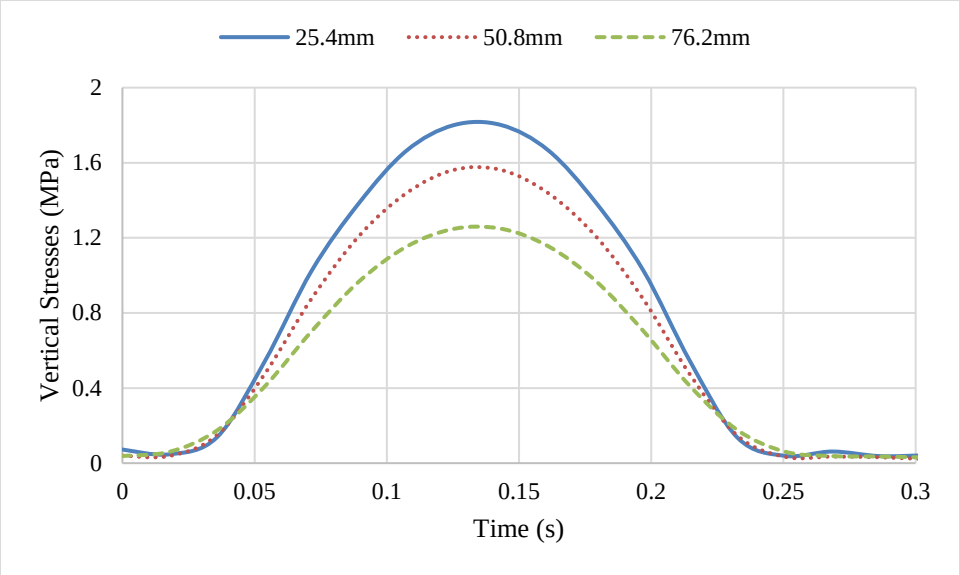

Figure 5 Stress magnitudes and pulses under moving load at different depths at 8km/h and 25°C

Table 3 presents the electric power output generated by the energy module located at 25.4 mm, 50.8 mm, and 76.2 mm under pavement surface. Compared to the embedment at 50.8 mm under pavement surface, the power output increased by 1-8% depending on the temperatures and horizontal locations of energy modules when the energy module was buried 25.4 mm under pavement surface. The embedment at 76.2 mm under pavement surface resulted in 9-20% reduction in electric power output.

Table 3 Electric power output generated by the 1-inch energy module placed at different depths (unit: mW per energy module)

Location of	**Under 25.4 mm**		**Under 50.8 mm**		**Under 76.2 mm**	
Energy Module	**25°C**	**40°C**	**25°C**	**40°C**	**25°C**	**40°C**

Edge Rib	932	922	859	858	685	703
Center Rib	756	758	739	752	655	683

4.4 Effect of Thickness of Energy Module

It was expected that the energy output could be enhanced by adding more layers of piezoelectric module. The flexible pavement structure with triple layers of the energy module, approximately 3-inch thickness, were simulated to estimate the energy output.

The electric power output was calculated on the basis of the vertical compressive stresses above individual layer of piezoelectric unit, as shown in Table 4. It is noted that, compared to the 1-inch thick energy module, the electric power output of the 3-inch module increased by 21-330% depending on the horizontal locations, temperature, and speed. However, the material costs would also increase threefold, which leads to a reduction in economic benefits of piezoelectric energy harvester.

Table 4 Electric power output generated by the 3-inch energy module

(unit: mW per energy module)

Location of	**8 km/h**		**48 km/h**	
Energy Module	**25°C**	**40°C**	**25°C**	**40°C**
Edge Ribs	1749	1765	9228	9720
Center Ribs	893	941	4930	5181
Besides Tire	45	53	47	53

4.5 Effect of Aircraft Wheel Configuration

Dual wheel and dual tandem are the two major categories of aircraft gear configurations. The compressive stresses at top of energy module and pavement responses under dual tandem were estimated and compared to those under dual wheels. The simulated aircraft speeds were 8 km/h and 48 km/h and the temperature was 25°C. The tire inflation pressure and tire load of landing gear were 1.57 MPa and 232 kN, which were the tire inflation pressure and take-off gross aircraft weight of B747-400 extracted from FAA Rigid and Flexible Iterative Elastic Layer Design (FAARFIELD) program (FAA, 2009).

Figure 6 illustrates the loading pulses of compressive stresses on top of the energy module under the landing gear of dual tandem. Negligible differences of compressive stresses and load pulses were observed as the two axles of dual tandem passing over the pavement surface. The results suggested that the vertical compressive stresses under the landing gears of dual tandem could be seen as those under two dual wheels while calculating energy power output.

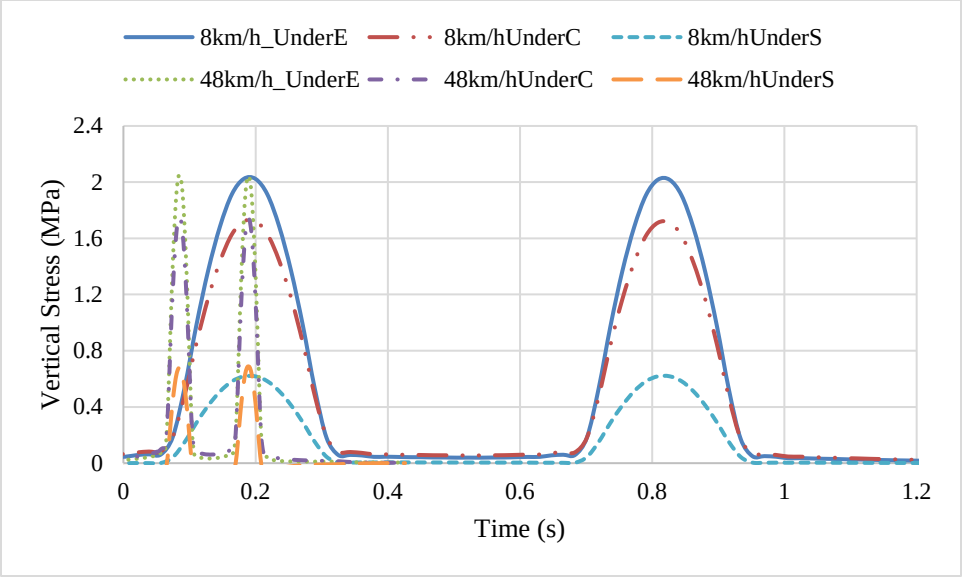

Figure 6 Stress pulses under dual tandem wheels at 25ºC

The electric power output was calculated based on the vertical compressive stresses and loading frequency from Figure 6. Table 5 presents the power output generated by the landing gear of dual tandem with energy module buried at different horizontal locations. It shows the remarkable increase in power output induced by the landing gears of dual tandems because of the two peaks of vertical compressive stresses.

Table 5 Electric power output under the landing gear of dual tandem (unit: mW per energy module)

Location of	**8 km/h**		**48 km/h**	
Energy Module	**25°C**	**40°C**	**25°C**	**40°C**
Edge Ribs	2855	2843	17546	17438

Center Ribs	2436	2485	14499	14687
Besides Tire	81	84	1435	1461

4.6 Effect of Aircraft Loads

Different magnitudes of tire loads were considered to investigate the relationship between vertical compressive stresses on top of energy module and tire loads applied on pavement structure. The take-off weights of A320-200 and B737-800 and the maximum landing weight of B737-800 were simulated. The tire inflation pressure was 1.40 MPa. The corresponding tire loads were 154 kN, 172 kN, and 185 kN, respectively. Figure 7 shows the positive linear relationship between the compressive stresses at top of energy module and the tire loadings at 8 km/h. The correlation could be used to estimate the compressive stresses at top of energy module under different magnitudes of aircraft tire loads with similar tire inflation pressure.

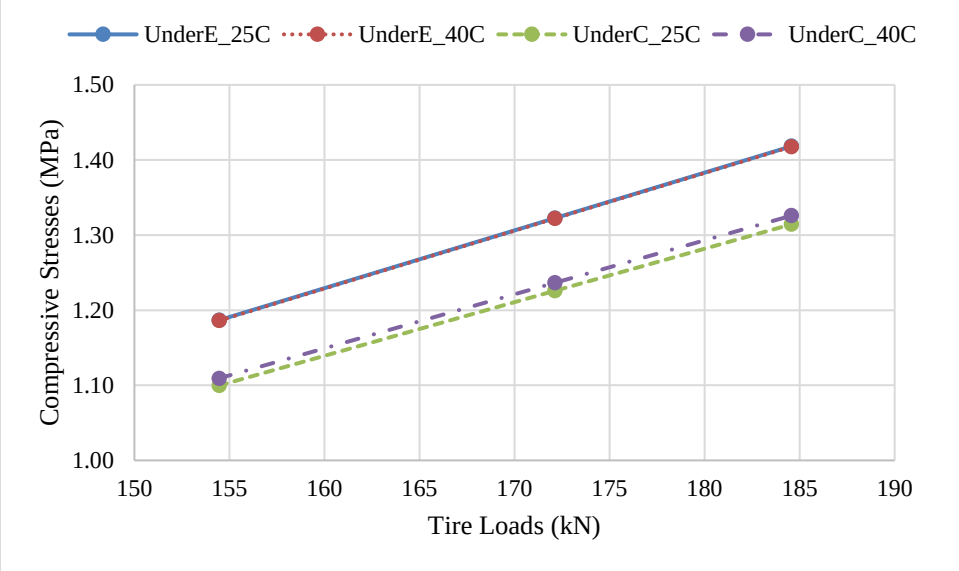

Figure 7 Compressive stresses under different tire loads at 8 km/h

The electric power output under different tire loads at 8 km/h was listed in Table 6. It indicated that the power output increased by 24% and 42% when the tire loads increased from 154 kN to 172 kN and 185 kN, respectively. A linear relationship between electric power output and tire loads was fitted based on the analysis results, which could be utilized to estimate electric energy outputs for other tire loads.

Table 6 Electric power output under different tire loads

(unit: mW per energy module)

Location of Energy Module	**154 kN**		**172 kN**		**185 kN**	
	25°C	**40°C**	**25°C**	**40°C**	**25°C**	**40°C**
Edge Ribs	859	858	1063	1062	1220	1219
Center Ribs	739	752	915	931	1050	1068

Section 5: Effect of Energy Harvester on Pavement Responses

For flexible pavements, fatigue cracking and rutting are major load-induced mechanical failures of pavement structure. In the study, pavement responses at critical locations in flexible pavement structure were used to investigate the impacts of piezoelectric energy harvester on structural responses. The horizontal tensile strains at the bottom of asphalt layer were estimated to evaluate the bottom-up cracking in pavement structure. To investigate the shear failure of flexible pavement, the near-surface shear strains were estimated. The vertical compressive strains at the top of subgrade were calculated to evaluate the permanent deformation of subgrade.

Table 7 summarizes the maximum horizontal strains at the bottom of asphalt concrete layer, maximum near-surface shear strains, and maximum compressive strains on the top of subgrade in pavement structure without and with the 1-inch energy module. The simulated aircraft speeds were 8 km/h, 48 km/h, and 96 km/h. The pavement temperatures of 25°C and 40°C were considered in the FE model. It indicates that the energy module increased the horizontal tensile strains at the bottom of AC layer and decreased the compressive strains at the top of subgrade slightly. The results are consistent with the expectation that the embedment of energy module would cause smaller deformation in asphalt concrete layer or on top of subgrade because of the greater stiffness of energy module. The negative effects of energy module on the horizontal strains at the bottom of asphalt concrete layer was not significant. However,

the energy module resulted in the increase of near-surface shear strains when the energy module was placed under the edge ribs of the tires. It is noted that the locations of the critical shear strains near pavement surface varied depending on the embedment location of energy module and temperature.

Table 7 Pavement responses at critical points with 1-inch thick energy module (unit: microstrain)

Speed	Location	25 °C			40 °C		
		Tensile strain at bottom of AC	**Near-surface shear strain**	**Compressive strain on top of subgrade**	**Tensile strain at bottom of AC**	**Near-surface shear strain**	**Compressive strain on top of subgrade**
8km/h	Without	205	176	248	350	488	383
	Edge	2%	25%	-2%	6%	15%	-1%
	Center	2%	-1%	-4%	5%	-1%	-2%
48km/h	Without	151	130	212	243	293	314
	Edge	2%	25%	-3%	8%	24%	-1%
	Center	2%	0%	-3%	10%	0%	-2%
96km/h	Without	142	124	211	220	251	304
	Edge	4%	25%	-3%	7%	23%	-4%
	Center	4%	-1%	-4%	7%	0%	-5%

The critical pavement responses and changes induced by the embedment of 3-inch thick energy module compared to the responses with 1-inch thick energy module were summarized in Table 8. The aircraft speeds of 8 km/h and 48 km/h and the pavement temperatures of 25°C and 40°C were taken into consideration. It was suggested that the pavement responses, especially near-surface shear strains, decreased as the energy module was placed at deeper locations in pavement structure.

Table 8 Pavement responses at critical locations with 3-inch thick energy module

(unit: microstrain)

Speed	Location	Tensile strain at bottom of AC	Near-surface shear strain	Compressive strain on top of subgrade	Tensile strain at bottom of AC	Near-surface shear strain	Compressive strain on top of subgrade
8km/h	Without	205	176	248	350	488	383
	Edge	2%	13%	-4%	1%	9%	-4%
	Center	2%	-2%	-6%	-3%	1%	-6%
48km/h	Without	151	130	212	243	293	314
	Edge	-2%	11%	-5%	2%	8%	-5%
	Center	-1%	-2%	-5%	-6%	-3%	-6%

It is expected that pavement responses varied with pavement depth. The changes of pavement responses when the 1-inch energy module was embedded at different depths were listed in Table 9. It indicated that near-surface shears strains were impacted significantly by the depths of embedment compared to horizontal strains at the bottom of AC layer and compressive strains on the top of subgrade. As the depth of energy module increased, the increase of near-surface shear strain caused by the embedment of energy module decreased.

Table 9 Pavement responses with 1-inch energy module placed at different pavement depths (unit: microstrain)

Locations of Energy Module	25ºC			40ºC		
	Horizontal tensile strain at the bottom of AC	Near-surface shear strain	Compressive strain on the top of subgrade	Horizontal tensile strain at the bottom of AC	Near-surface shear strain	Compressive strain on the top of subgrade

Without Energy Module		205	176	248	350	488	383
25.4mm	Edge	3%	38%	-3%	8%	26%	-3%
	Center	2%	2%	-6%	6%	2%	-5%
50.8mm	Edge	2%	25%	-2%	6%	15%	-1%
	Center	2%	-1%	-3%	5%	-1%	-2%
76.2mm	Edge	2%	10%	-1%	6%	0%	1%
	Center	1%	-14%	-2%	2%	-30%	-1%

The analysis results indicated that near-surface shear strains were the dominant responses for potential damage of flexible pavement structure with the energy module. Therefore, the shear resistance of pavement surface course need be enhanced when piezoelectric energy harvesters are buried in airfield pavement structure.

Section 6: Conclusions

This study investigated the feasibility of piezoelectric energy harvesting at airfield pavement. The FE model was developed to predict compressive stress pulses on energy harvester under different aircraft tire loading conditions, which were used to calculate power output potential. The impact of energy module on critical pavement responses was also analyzed considering different pavement failure mechanisms.

Aircraft load and speed are vital factors affecting power output. The power output increased as the aircraft load or speed increased. However, for energy output, the positive impact of aircraft speed may be eliminated by the short loading period at high speeds. It was found that the embedment depth and horizontal locations had significant influence on vertical compressive stresses on top of piezoelectric energy harvester. This indicates that aircraft wandering will also affect the energy output.

On the other hand, the embedment of energy module had negligible influence on horizontal tensile strains at the bottom of AC layer and compressive strains on the top of subgrade. However, the near-surface shear strains increased when the edge ribs of tire were loaded on energy module.

The energy output of piezoelectric energy module was estimated based on one prototype of energy module proposed in previous study. Different designs of piezoelectric transducer and energy module will affect the energy output. In future

work, the optimized design and embedment location of energy module need be studied considering both the generated energy output and the impact on pavement responses.

It is expected that the piezoelectric energy harvested from pavement may not be applicable for power grid applications. It is more practical to directly use the harvested energy in the airport for lighting and sensor applications. The piezoelectric energy harvesting system can provide distributed energy source in the airfield and lead to the development of smart infrastructure.

References

Anton, S. R., and H. A. Sodano. 2007. "A review of power harvesting using piezoelectric materials (2003–2006)." *Smart materials and Structures*, 16(3), R1.

Brady, C. 1999. *The Boeing 737 Technical Guide*.

Cobbold, R. S. 2006. *Foundations of biomedical ultrasound*, Oxford University Press.

Dassault Systèmes. "ABAQUS version 6.13."Waltham, MA.

Federal Aviation Administration. 2009. "Advisory Circular: Airport Pavement Design and Evaluation ".

Federal Aviation Administration (FAA). "FAARFIELD 1.42."Washington, DC.

Guan, M., and W.-H. Liao. 2008. "Characteristics of Energy Storage Devices in Piezoelectric Energy Harvesting Systems." *Journal of intelligent material systems and structures*, 19(6), 671-680.

Hadjipaschalis, I., A. Poullikkas, and V. Efthimiou. 2009. "Overview of Current And Future Energy Storage Technologies for Electric Power Applications." *Renewable and sustainable energy reviews*, 13(6-7), 1513-1522.

Jasim, A. F., H. Wang, G. Yesner, A. Safari, and P. Szary. 2019. "Performance Analysis of Piezoelectric Energy Harvesting in Pavement: Laboratory Testing and Field Simulation."

Jiang, X., Y. Li, J. Wang, and J. Li. 2014. "Electromechanical Modeling and Experimental Analysis of a Compression-Based Piezoelectric Vibration Energy Harvester." *International Journal of Smart and Nano Materials*, 5(3), 152-168.

Miclea, C., C. Tanasoiu, L. Amarande, M. Cioangher, L. Trupina, C. T. Miclea, and C. David. "Temperature Dependence of the Main Piezoelectric Parameters of a Nb-Li Doped PZT Ceramic." *Proc., 2006 International Semiconductor Conference, CAS 2006, September 27, 2007 - September 29, 2007*, Institute of Electrical and Electronics Engineers Inc., 279-282.

Ottman, G. K., H. F. Hofmann, A. C. Bhatt, and G. A. Lesieutre. 2002. "Adaptive Piezoelectric Energy Harvesting Circuit for Wireless Remote Power Supply." *IEEE Transactions on power electronics*, 17(5), 669-676.

Park, S. W., and Y. R. Kim. 1999. "Interconversion between Relaxation Modulus and Creep Compliance for Viscoelastic Solids." *J. Mater. Civ. Eng.*, 11(1), 76-82.

Rolland, E. 2009. "Tire Pressure Test Effect on Pavement." Airbus High Tire Pressure Workshop (in CD), Toulouse, France.

Roshani, H., and S. Dessouky. 2015. "Feasibility Study to Harvest Electric Power from Highway Pavements using Laboratory Investigation." *Department of Civil and Environmental Engineering University of Texas at San Antonio*.

Roshani, H., S. Dessouky, A. Montoya, and A. T. Papagiannakis. 2016. "Energy Harvesting from Asphalt Pavement Roadways Vehicle-Induced Stresses: A Feasibility Study." *Applied Energy*, 182, 210-218.

Roshani, H., P. Jagtap, S. Dessouky, A. Montoya, and A. T. Papagiannakis. 2018. "Theoretical and Experimental Evaluation of Two Roadway Piezoelectric-Based Energy Harvesting Prototypes." *J. Mater. Civ. Eng.*, 30(2).

Roundy, S., P. K. Wright, and J. Rabaey. 2003. "A study of low level vibrations as a power source for wireless sensor nodes." *Computer Communications*, 26(11), 1131-1144.

Sodano, H. A., D. J. Inman, and G. Park. 2005. "Generation and Storage of Electricity from Power Harvesting Devices." *Journal of Intelligent material systems and structures*, 16(1), 67-75.

Wang, H., M. Li, and N. Garg. 2015. "Airfield Flexible Pavement Responses Under Heavy Aircraft and High Tire Pressure Loading." *Transp. Res. Rec.*, 2501, 31-39.

Wang, H., M. Li, and N. Garg. 2016. "Investigation of Shear Failure in Airport Asphalt Pavements under Aircraft Ground Manoeuvring." *Road Mater Pavement*, 18(6), 1288-1303.

Whiteman, A., D. Bannard, T. Smalinsky, I. Korovesi, J. Plante, and T. DeVault. 2015. *Renewable Energy as an Airport Revenue Source*.

Xiang, H. J., J. J. Wang, Z. F. Shi, and Z. W. Zhang. 2013. "Theoretical Analysis of Piezoelectric Energy Harvesting from Traffic induced Deformation of Pavements." *Smart Materials and Structures*, 22(9), 095024.

Xiong, H. 2014. "Piezoelectric Energy Harvesting on Public Roadways." Ph.D Dissertation, Virginia Polytechnic Institute and State University, VA.

Zhang, Z., H. Xiang, and Z. Shi. 2016. "Modeling on Piezoelectric Energy Harvesting from Pavements under Traffic Loads." *Journal of Intelligent Material Systems and Structures*, 27(4), 567-578.